



## UvA-DARE (Digital Academic Repository)

### Unraveling immunity in chronic lymphocytic leukemia

*Therapeutic implications*

de Weerd, I.

**Publication date**

2020

**Document Version**

Other version

**License**

Other

[Link to publication](#)

**Citation for published version (APA):**

de Weerd, I. (2020). *Unraveling immunity in chronic lymphocytic leukemia: Therapeutic implications*. [Thesis, fully internal, Universiteit van Amsterdam].

**General rights**

It is not permitted to download or to forward/distribute the text or part of it without the consent of the author(s) and/or copyright holder(s), other than for strictly personal, individual use, unless the work is under an open content license (like Creative Commons).

**Disclaimer/Complaints regulations**

If you believe that digital publication of certain material infringes any of your rights or (privacy) interests, please let the Library know, stating your reasons. In case of a legitimate complaint, the Library will make the material inaccessible and/or remove it from the website. Please Ask the Library: <https://uba.uva.nl/en/contact>, or a letter to: Library of the University of Amsterdam, Secretariat, Singel 425, 1012 WP Amsterdam, The Netherlands. You will be contacted as soon as possible.

## DISTINCT IMMUNE COMPOSITION IN LYMPH NODE AND PERIPHERAL BLOOD OF CLL PATIENTS IS RESHAPED DURING VENETOCLAX TREATMENT

Iris de Weerd<sup>1,2\*</sup>, Tom Hofland<sup>1,2\*</sup>, Renate de Boer<sup>1,2</sup>, Johan Dobber<sup>1</sup>, Julie Dubois<sup>1</sup>, Denise van Nieuwenhuize<sup>1,2</sup>, Mehrdad Mobasher<sup>4</sup>, Fransien de Boer<sup>5</sup>, Mels Hoogendoorn<sup>6</sup>, Gerjo A. Velders<sup>7</sup>, Marjolein van der Klift<sup>8</sup>, Ester B.M. Remmerswaal<sup>2</sup>, Frederike J. Bemelman<sup>9</sup>, Carsten U. Niemann<sup>10</sup>, Sabina Kersting<sup>11</sup>, Mark-David Levin<sup>12</sup>, Eric Eldering<sup>2,3</sup>, Sanne H. Tonino<sup>1,3+</sup> and Arnon P. Kater<sup>1,3+</sup>

<sup>1</sup>Department of Hematology, Amsterdam UMC, University of Amsterdam, Amsterdam

<sup>2</sup>Department of Experimental Immunology, Amsterdam UMC, University of Amsterdam, Amsterdam

<sup>3</sup>Lymphoma and Myeloma Center Amsterdam, LYMMCARE, Amsterdam

<sup>4</sup>Genentech Inc, South San Francisco, CA

<sup>5</sup>Internal Medicine, Ikazia Hospital, Rotterdam

<sup>6</sup>Internal Medicine, Medical Center Leeuwarden, Leeuwarden

<sup>7</sup>Department of Internal Medicine, Gelderse Vallei Hospital, Ede

<sup>8</sup>Department of Internal Medicine, Amphia Hospital, Breda

<sup>9</sup>Renal Transplant Unit, Amsterdam UMC, University of Amsterdam, Amsterdam

<sup>10</sup>Department of Haematology, Rigshospitalet, Copenhagen University Hospital, Copenhagen

<sup>11</sup>Department of Hematology, Haga Hospital, the Hague

<sup>12</sup>Department of Internal Medicine, Albert Schweitzer Hospital, Dordrecht

\*These authors contributed equally

+Shared senior authorship

**ABSTRACT**

Morbidity and mortality due to immunosuppression remain among the foremost clinical challenges in chronic lymphocytic leukemia (CLL). Although immunosuppression is considered to originate within the lymph node (LN) microenvironment, alterations in T and natural killer (NK) cells have almost exclusively been studied in peripheral blood (PB). Whereas chemoimmunotherapy further deteriorates immune function, novel targeted agents like the B-cell lymphoma 2 inhibitor venetoclax potentially spare nonmalignant lymphocytes; however, the effects of venetoclax on nonleukemic cells have not been explored. We address these unresolved issues using a comprehensive analysis of nonmalignant lymphocytes in paired LN and PB samples from untreated CLL patients, and by analyzing the effects of venetoclax-based treatment regimens on the immune system in PB samples from previously untreated and relapsed/refractory patients. CLL-derived LNs contained twice the amount of suppressive regulatory T cells ( $T_{regs}$ ) and CLL supportive follicular T helper ( $T_{fh}$ ) cells compared with PB. This was accompanied by a low frequency of cytotoxic lymphocytes. The expression of PD-1 by  $CD8^+$  T cells was significantly higher in LN compared with PB. Venetoclax-based treatment led to deep responses in the majority of patients, but also to decreased absolute numbers of B, T, and NK cells.  $T_{fh}$  cell,  $T_{reg}$ , and PD-1 $^+$   $CD8^+$  T cell numbers were reduced more than fivefold after venetoclax-based therapy, and overproduction of inflammatory cytokines was reduced. Furthermore, we observed restoration of NK cell function. These data support the notion that the immunosuppressive state in CLL is more prominent within the LN. Venetoclax-based regimens reduced the immunosuppressive footprint of CLL, suggesting immune recovery after the elimination of leukemic cells.

## INTRODUCTION

Chronic lymphocytic leukemia (CLL) is accompanied by considerable immunosuppression, which results in an increased risk for infections and secondary malignancies<sup>1,2</sup>. Immune disruptions are thought to arise from interactions between CLL cells and the immune system. These interactions provide a supportive microenvironment for CLL cells and allow escape from immunosurveillance<sup>1-3</sup>. CLL cells actively shape a supportive immune environment that results in progressive abnormalities in the myeloid, T, and natural killer (NK) cell compartment of CLL patients<sup>3,4</sup>. One result of such T-cell alterations is the elevation of CD4<sup>+</sup> and CD8<sup>+</sup> T-cell numbers, resulting in a decreased CD4/CD8 ratio<sup>5</sup>. CD4<sup>+</sup> T cells are skewed toward a T helper 2 (T<sub>H</sub>2) cell profile and are considered to support CLL cells via cytokines, chemokines, and membrane-bound factors<sup>6-8</sup>. Regulatory CD4<sup>+</sup> T cells (T<sub>regs</sub>) suppress cellular immune responses and experimental evidence<sup>9,10</sup>, as well as the observation that T<sub>reg</sub> expansion is more prominent in patients with higher CLL loads<sup>11,12</sup>, indicates that CLL cells actively recruit T<sub>regs</sub>. Although CD8<sup>+</sup> T cells of CLL patients produce high levels of interferon- $\gamma$  (IFN- $\gamma$ ) and tumor necrosis factor- $\alpha$ , the overexpression of inhibitory molecules, such as PD-1, is associated with reduced proliferative capacity and cytotoxicity<sup>13-16</sup>. NK cell functionality is also impaired in CLL, particularly with regard to degranulation and cytotoxicity<sup>17,18</sup>.

Similar to other B-cell lymphomas, such as follicular lymphoma, the lymph node (LN) microenvironment in CLL is thought to be the predominant site of interaction between the malignant cells and tumor-associated and tumor-specific immune cells<sup>19</sup>. However, data on immune abnormalities in CLL patients are primarily obtained from peripheral blood (PB) studies, and little is known about the composition of nonmalignant lymphocytes in LN tissue or how this relates to PB.

Chemoimmunotherapy (especially bendamustine and fludarabine) has detrimental effects on the number and function of T cells, further compromising immune function in CLL patients<sup>20,21</sup>. Although experience so far indicates that most novel targeted therapeutic strategies do not have such unfavorable effects on T cells, targeted agents may also influence the immune system of CLL patients<sup>22</sup>. The Bruton tyrosine kinase (BTK) inhibitor ibrutinib alters T, NK, and myeloid cell function, which may result, in part, from off-target inhibition of other kinases, such as interleukin-2 (IL-2)-inducible T-cell kinase<sup>23-26</sup>. However, some of these T-cell alterations have also been observed in patients treated with the more selective BTK inhibitor acalabrutinib, which does not inhibit inducible T-cell kinase, implying that on-target effects via the eradication of CLL cells also eventually affect the nonmalignant immune system<sup>27</sup>.

Venetoclax, an inhibitor of the antiapoptotic protein B-cell lymphoma 2 (Bcl-2), is highly effective in CLL, even as monotherapy<sup>28</sup>. High rates of minimal residual disease (MRD) negativity and low rates of progression are observed with venetoclax treatment in combination with anti-CD20 monoclonal antibodies, such as obinutuzumab<sup>29-32</sup>. The effects of venetoclax on nonmalignant lymphocytes have not been investigated in patient samples. Although CLL cells rely heavily on

Bcl-2 for their survival, other leukocytes also depend on Bcl-2 to varying degrees and, thus, may be affected by venetoclax-based treatment<sup>33,34</sup>.

Understanding the effects of novel treatment regimens on the immune system is particularly important considering the fact that infections remain a leading cause of morbidity and mortality in CLL<sup>35,36</sup>. In addition, knowledge about how venetoclax impacts lymphocytes may be valuable in designing future combination strategies and shed light on possible risks associated with long-term treatment. Eradication of the malignant clone potentially allows recovery of immune responses and, thus, immunosurveillance.

To characterize the immunosuppressive footprint of CLL, we first studied the immune composition of the PB and LN compartments in untreated progressive CLL patients. We found increased numbers of tumor-supporting lymphocyte subsets and decreased numbers of cytotoxic lymphocyte subsets in the LN compared with PB, indicating an immunosuppressive environment within the LN tissue. Second, we analyzed the effect of venetoclax-based treatment on the phenotype and function of nonmalignant lymphocytes in 2 trial cohorts. Venetoclax-based treatment led to significant reductions in characteristic immunosuppressive features of CLL but did not affect the functionality of T and NK cells, suggestive of immune recovery after venetoclax-based treatment.

## METHODS

### Patient material

PB and fine-needle LN biopsies were collected from CLL patients in 2 phase 2 clinical trials performed by the Dutch-Belgian Cooperative Trial Group for Hematology Oncology (HOVON): the HOVON139 trial (Netherlands Trial Registry ID: NTR6043) and the HOVON141 trial (Netherlands Trial Registry ID: NTR6249). Healthy control (HC) PB and LN samples were collected from patients undergoing renal transplantation, as described previously<sup>37</sup>. During sample collection, HCs had received no immunosuppressive medication other than 1 administration of anti-CD25 monoclonal antibody. For an overview of donor characteristics see Table 1. The studies were approved by the medical ethics committee at the Amsterdam UMC. Written informed consent from all subjects was obtained in accordance with the Declaration of Helsinki.

### Study design

Previously untreated CLL patients were enrolled in the HOVON139 GIVE trial (NTR6043)<sup>30</sup>. The treatment regimen consisted of preinduction with obinutuzumab (3000 mg in cycle 1 and 1000 mg in cycle 2), induction with combined venetoclax (ramp up to 400 mg) and obinutuzumab (1000 mg; cycles 3-8), and venetoclax monotherapy (400 mg; cycles 9-14 or longer).

PB mononuclear cells (PBMCs) were collected before the start of the trial, as well as after cycle 2 and after cycle 14 (or ~1 year) of treatment, and were used directly or cryopreserved as described earlier<sup>38</sup>. Core LN biopsies were collected at baseline and used directly.

**Table 1. Patient characteristics.**

	HC	HOVON139 Baseline PB	HOVON139 Baseline LN	HOVON139 1 year PB	HOVON141 Baseline PB	HOVON141 1 year PB
N	10	41	28	11	10	10
Sex (% male)	50	75.7	80.8	81.8	30.0	30.0
Age (years)	63 (45-78)	71 (57-80)	71 (57-79)	71.5 (60-78)	68 (52-76)	68 (52-76)
CMV (% positive)	83	41	48	64	Not known	Not known
ALC (*10 <sup>9</sup> /L)	Not known	98.6 (3.5-420.7)	97.3 (18.0-399.0)	4.8 (2.8-9.9)	129.8 (20.0-248.9)	4.8 (3.9-7.6)
TTFT (months)	N/A	28.2 (0.7-244.6)	28.1 (0.7-244.6)	18.9 (1.7-244.6)	Not known	Not known
Prior treatment (number)	N/A	-	-	-	1 (1-3)	1 (1-3)
Prior chemotherapy (%)	N/A	-	-	-	100	100
TTT (months)	N/A	N/A	N/A	N/A	42.8 (13.8-141.8)	42.8 (13.8-141.8)
Rai stage (% III-IV)	N/A	57.1	44.0	36.4	80	80
IgVH status (% U-CLL)	N/A	55.9	55.6	27.3	40	40

Data are presented as median (range). ALC: absolute leukocyte count; TTF: time to first treatment; N/A: not applicable; TTT: time from last treatment to current treatment; U-CLL: CLL with unmutated immunoglobulin heavy chains.

Patients with relapsed or refractory CLL were enrolled in the HOVON141 Vision trial (NTR6249). The treatment regimen consisted of ibrutinib monotherapy (420 mg days 1-28; cycle 1 and 2), followed by combined venetoclax (ramp up to 400 mg) and ibrutinib (420 mg; cycles 3-15).

PBMCs were collected before the start of the trial, as well as after cycle 2 and after cycle 14 (or ~1 year) of treatment, and cryopreserved. The second time point was chosen to match the number of venetoclax cycles received in the HOVON139 trial.

Cells were incubated with monoclonal antibodies for surface staining for 20 minutes at 4°C. Monoclonal antibodies used are listed in Supplementary Table 1 (online version). Cells were then washed, fixed, and stained intracellularly for 30 minutes at 4°C using a Foxp3/Transcription Factor Staining Buffer Set (Thermo Fisher Scientific, Waltham, MA). Reference values are derived from the Netherlands Society for Clinical Chemistry and Laboratory Medicine

### **Lymphocyte activation**

Cells were stimulated with phorbol myristate acetate (PMA; 10 ng/mL) and ionomycin (1 µg/mL) for 4 hours in the presence of Brefeldin A (10 µg/mL; all from Sigma-Aldrich, St. Louis, MO), GolgiStop (BD Biosciences, Franklin Lakes, NJ), and CD107a FITC (Thermo Fisher Scientific). Cells were washed, and surface staining was performed as described above. Fixation and intracellular staining were performed using a BD Cytotfix/Cytoperm Fixation/Permeabilization Solution kit (BD Biosciences).

### **Flow cytometry**

Samples were measured on a BD FACSCanto II or a BD LSRFortessa cytometer (both from BD Biosciences). Samples were analyzed with FlowJo v10.

### **Statistical analyses**

Data were checked for normality with the D'Agostino-Pearson normality test and analyzed using a Wilcoxon matched-pairs signed-rank test, 1-way analysis of variance (ANOVA), or Pearson correlation analysis. Statistical analyses were performed with GraphPad Prism v7.

## **RESULTS**

### **Fewer cytotoxic T and NK cells in the LN than in the PB**

We compared lymphocyte composition between the LN and PB from previously untreated CLL patients and from HCs (gating strategy is shown in Supplementary Figure 1).

The percentage of CLL cells was lower in the LN than in the PB (92.3% of lymphocytes in PB vs 82.8% in LN), because relative T-cell numbers were increased in the LN of CLL patients (5.1% in PB vs 13.2% in LN; Figure 1A-B). On the other hand, T cells were less frequent in the LN than in the PB (52.7% vs 75.12%, respectively) in HCs.

In CLL patients and HCs, the T-cell population in the LN is dominated by CD4<sup>+</sup> T cells at the expense CD8<sup>+</sup> T cells (Figure 1C). In addition to ( $\alpha\beta$ ) CD8<sup>+</sup> T cells, V $\delta$ 1 and V $\delta$ 2 T cells are the most common T-cell populations with anti-tumor properties<sup>39</sup>. In contrast to  $\alpha\beta$  T cells, both V $\delta$ 1 and V $\delta$ 2 T cell frequencies were more than fourfold lower in the LN than in the PB in CLL patients (Figure 1D-E).

The proportion of NK cells in the LN was significantly lower compared with the PB in CLL patients and HCs (Figure 1F). Within the NK cell compartment, CD56<sup>dim</sup> cells with a cytotoxic potential are distinguished from CD56<sup>bright</sup> cells that have a higher proliferative and cytokine-producing capacity<sup>40</sup>. In patients with CLL and HCs, the majority (>90%) of PB NK cells were CD56<sup>dim</sup> NK cells (Supplementary Figure 2A-C). CD56<sup>bright</sup> NK cells made up a minority of the NK cells in the PB but a considerable fraction (~83%) of the LN NK cells, although this was less pronounced (~56%) in CLL patients than in HCs.

Thus, within the LN, CLL cells are accompanied primarily by CD4<sup>+</sup> T cells and relatively few (cytotoxic) T and NK cells.

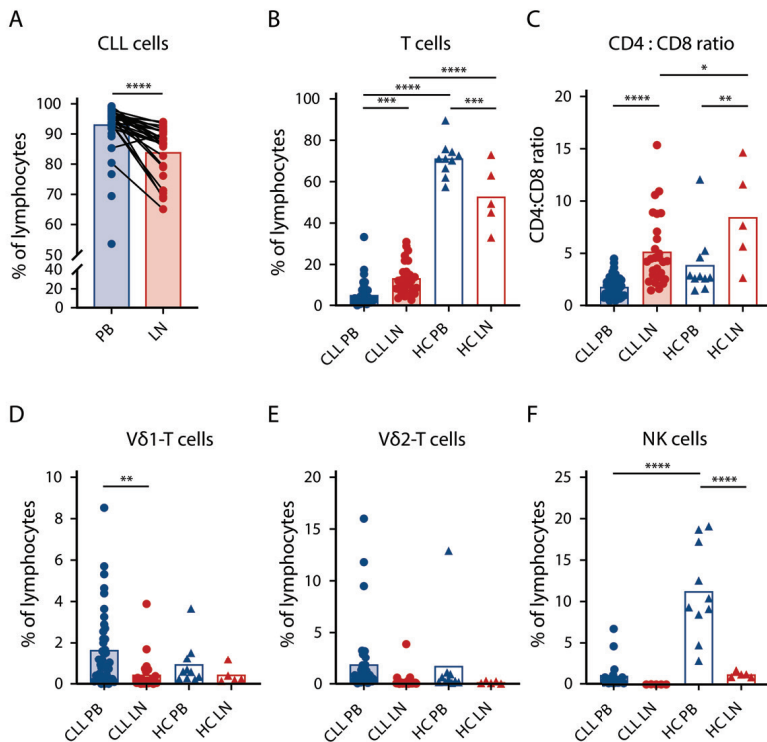


**Figure 1. Few cytotoxic lymphocytes in the LN of CLL patients.** Lymphocyte analysis in PB and LN samples from untreated CLL patients (PB, n = 42; LN, n = 28) and HCs (PB, n = 10; LN, n = 5) by flow cytometry. Percentage of CLL (CD5<sup>+</sup>CD19<sup>+</sup>) cells (A) and T (CD3<sup>+</sup>) cells (B) within lymphocytes. (C) Ratio of CD4<sup>+</sup>/CD8<sup>+</sup> T cells. Percentage of V $\delta$ 1<sup>+</sup> cells (D) and V $\delta$ 2<sup>+</sup> cells (E) within T cells. (F) Percentage of NK (CD56<sup>bright</sup> and CD16<sup>+</sup>) cells within lymphocytes (CLL PB, n = 21; CLL LN, n = 5). Data are presented as mean (bar) and individual patients (circles and triangles). \*P < .05, \*\*P < .01, \*\*\*P < .001, \*\*\*\*P < .0001, Wilcoxon matched-pairs signed-rank test (A), 1-way ANOVA followed by Sidak's multiple-comparisons test (B-F).



**Immunosuppressive T-cell composition in CLL LN**

Next, we investigated the subset distribution of T cells in the LN. CD4<sup>+</sup> T cells can differentiate into follicular T helper (T<sub>fh</sub>) cells that provide support to healthy B cells, and are similarly instrumental for CLL cell support<sup>7,41</sup>. LNs of CLL patients and HCs contained 3 times more T<sub>fh</sub> cells compared with the PB (Figure 2A). We could not replicate previous reports of elevated T<sub>fh</sub> cell numbers in the PB of CLL patients with advanced disease<sup>42,43</sup>.

CLL cells have been reported to promote T<sub>reg</sub> differentiation<sup>9,10,12</sup>. T<sub>regs</sub> were more frequent in the LN than in the PB of CLL patients (6.8% of CD4<sup>+</sup> T cells in PB vs 11.5% in LN), whereas in HCs, T<sub>regs</sub> were more prevalent in PB than in the LN (5.9% in PB vs 1.8% in LN; Figure 2B). The percentage of T<sub>regs</sub> in the LN correlated positively with the absolute leukocyte count in the PB of CLL patients (Figure 2C).

CD4<sup>+</sup> and CD8<sup>+</sup> T cells can be subdivided into naive T cells, central memory T cells, effector memory T cells, and RA-expressing effector memory T cells based on CD27 and CD45RA expression<sup>44</sup>. Although the differentiation status of CD4<sup>+</sup> T cells did not differ between LN and PB in CLL patients and HCs, the CD8<sup>+</sup> compartment in CLL patients consisted of a larger proportion of central memory T cells in the LN in comparison with the PB (37.2% of CD8<sup>+</sup> T cells in PB vs 60% in LN; Supplementary Figure 2D-E). RA-expressing effector memory T cells were less prevalent in the LN than in the PB in CLL patients (fivefold difference) and HCs (threefold difference; Supplementary Figure 2F-G). An important mechanism for negatively regulating the function of CLL CD8<sup>+</sup> T cells is through inhibitory molecules, such as PD-1<sup>15</sup>. Significantly more CD8<sup>+</sup> T cells expressed PD-1 in the LN (30.4%) than in the PB (12.4%) of CLL patients (Figure 2D).

In conclusion, the CLL LN shows increased frequencies of tumor-supportive T<sub>fh</sub> cells and T<sub>regs</sub> compared with the PB. Furthermore, there is a lower frequency of effector CD8<sup>+</sup> T cells and a higher PD-1 expression on remaining CD8<sup>+</sup> T cells in the CLL LN.

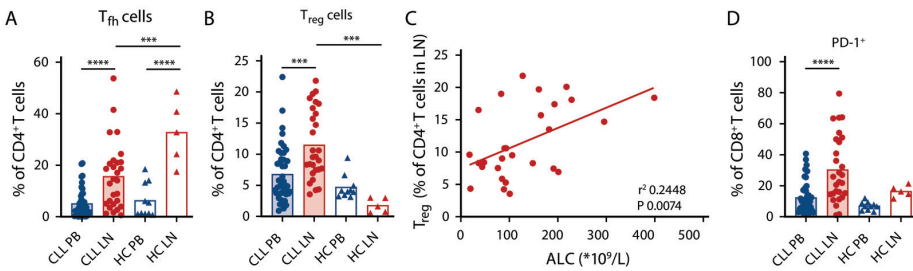


**Figure 2. CLL cells reside in an immunosuppressive context in the LN.** Lymphocyte analysis in PB and LN samples from untreated CLL patients (PB, n = 42; LN, n = 28) and HCs (PB, n = 10; LN, n = 5) by flow cytometry. Percentage of T<sub>fh</sub> (CXCR5<sup>+</sup>PD-1<sup>+</sup>) cells (A) and T<sub>regs</sub> (CD25<sup>+</sup>FoxP3<sup>+</sup>) (B) within CD4<sup>+</sup> T cells. (C) Correlation between the percentage of T<sub>regs</sub> of CD4<sup>+</sup> T cells in the CLL LN and the absolute leukocyte count (ALC). (D) Percentage of PD-1<sup>+</sup> cells within CD8<sup>+</sup> T cells. \*\*\*P < .001, \*\*\*\*P < .0001, 1-way ANOVA followed by Sidak’s multiple-comparisons test (A-B,D), Pearson correlation analysis (C).

### Reduced numbers of nonmalignant lymphocyte subsets after venetoclax and obinutuzumab treatment

To determine the effects of venetoclax treatment on nonmalignant lymphocytes, we studied paired PB samples obtained at baseline, after 2 months of preinduction with obinutuzumab, and at 1 year of treatment with venetoclax-obinutuzumab.

CLL cells were largely eliminated after 1 year of treatment (mean percentage within lymphocytes decreased from  $93.0\% \pm 4.5\%$  to  $0.1\% \pm 0.2\%$ ; Supplementary Figure 3A). The frequency of CLL cells presented is not derived from the simultaneously performed flow cytometry-based MRD analysis and likely overestimates the amount of CLL cells present as a result of less stringent criteria. MRD analysis during the trial demonstrated that, at this time point, 10 of these 11 patients had undetectable MRD ( $<10E^{-4}$ ), and the remaining patient was MRD intermediate-positive ( $>10E^{-4}$  and  $<10E^{-2}$ ), in line with our published interim analysis (MRD-intermediate-positive, 7.1%; MRD undetectable, 92.9%;  $n = 28$ )<sup>30</sup>.

We evaluated the absolute numbers of normal B, T, and NK cells after venetoclax-obinutuzumab treatment. The relative and absolute numbers of healthy B cells decreased after preinduction with obinutuzumab (Figure 3A; Supplementary Figure 3A). Absolute T-cell numbers were elevated in the majority of patients at baseline and after 2 months of treatment (mean T-cell number at baseline,  $3.4 \times 10^9/L \pm 2.6 \times 10^9/L$ ; reference values,  $0.7 \times 10^9/L$  to  $2.1 \times 10^9/L$ ). After 1 year of venetoclax-based treatment, the absolute number of CD4<sup>+</sup> T cells ( $0.5 \times 10^9/L \pm 0.2 \times 10^9/L$ ; reference values,  $0.3 \times 10^9/L$  to  $1.4 \times 10^9/L$ ) and CD8<sup>+</sup> T cells ( $0.2 \times 10^9/L \pm 0.1 \times 10^9/L$ ; reference values,  $0.2 \times 10^9/L$  to  $0.9 \times 10^9/L$ ) decreased (Figure 3B). The CD4/CD8 ratio and differentiation status of T cells did not change during therapy, indicating that T-cell reduction occurred across all subsets in CD4<sup>+</sup> and CD8<sup>+</sup> T cells (Supplementary Figure 3B-D), as well as that not all immune disturbances in CLL, like skewing of T-cell subsets, are restored after 1 year of venetoclax-based therapy. Unlike  $\alpha\beta$  T cells, the absolute number of V $\delta$ 1 and V $\delta$ 2 T cells remained stable during treatment (Supplementary Figure 3E-H).

The relative number of NK cells increased (from 0.7% to 8.0%; Supplementary Figure 3A), but the absolute number of NK cells decreased, during treatment (from  $0.5 \times 10^9/L \pm 0.3 \times 10^9/L$  to  $0.07 \times 10^9/L \pm 0.07 \times 10^9/L$ ; reference values,  $0.09 \times 10^9/L$  to  $0.6 \times 10^9/L$ ; Figure 3C). The CD56<sup>bright</sup>/CD56<sup>dim</sup> ratio increased after preinduction with obinutuzumab, perhaps as a result of the loss of CD56<sup>dim</sup> cells via activation-induced cell death, which is associated with obinutuzumab treatment (Figure 3D; Supplementary Figure 3I)<sup>45</sup>. After 1 year of venetoclax-based treatment, the CD56<sup>bright</sup>/CD56<sup>dim</sup> ratio recovered to the same range as baseline.

Taken together, combined treatment with venetoclax and obinutuzumab led to depletion of CLL cells and to a greater than threefold reductions in healthy B cells, T cells, and NK cells.

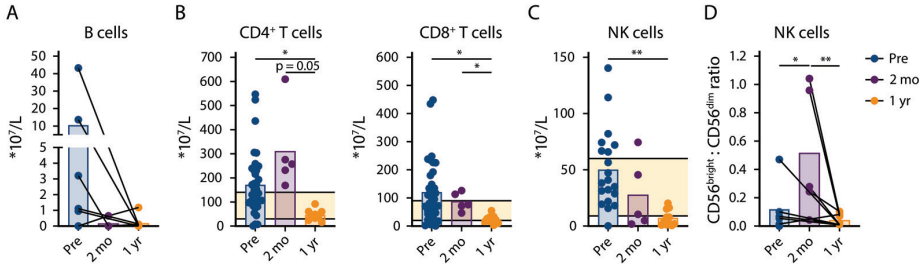


**Figure 3. Depletion of nonmalignant lymphocytes during venetoclax-obinutuzumab treatment.** Lymphocyte analysis in PB of patients at baseline (n = 36), after preinduction with obinutuzumab (n = 5), and after 1 year of treatment with venetoclax-obinutuzumab (n = 11) by flow cytometry. Absolute number of B cells (A) and CD4<sup>+</sup> and CD8<sup>+</sup> T cells (B) in PB. (C) Absolute number of NK (CD56<sup>bright</sup> and CD16<sup>+</sup>) cells in PB (baseline, n = 20). (D) Ratio of CD56<sup>bright</sup> (CD56<sup>bright</sup>CD16<sup>-</sup>)/CD56<sup>dim</sup> (CD56<sup>dim</sup>CD16<sup>+</sup>) cells (baseline, n = 6). Horizontal lines indicate reference values. \**P* < .05, \*\**P* < .01, 1-way ANOVA followed by Sidak’s multiple-comparisons test.

**Tumor-supportive T-cell subsets decline during venetoclax-obinutuzumab treatment**

We next investigated the phenotypical and functional differences of nonmalignant lymphocytes after venetoclax-obinutuzumab treatment. The frequencies of T<sub>h</sub> cells, T<sub>regs</sub>, and PD-1<sup>+</sup> CD8<sup>+</sup> T cells significantly decreased approximately sevenfold after venetoclax-based therapy, which is indicative of a reversal in the CLL immune signature (Figure 4A-C). None of these changes were apparent after obinutuzumab preinduction. Lymphocyte function before and after venetoclax-obinutuzumab was investigated by measuring immunoglobulin G (IgG) levels in plasma and by stimulating PBMCs with PMA/ionomycin.

Plasma IgG levels were low at baseline and did not increase after 1 year of treatment, in line with the low numbers of healthy B cells (mean IgG concentration after treatment, 5.8 g/L; reference values, 6-16 g/L; Figure 4D). Changes in T<sub>H</sub>1 cell cytokine production were ambiguous, because CD4<sup>+</sup> T cells produced significantly less IFN-γ, but IL-2 production increased, after PMA/ionomycin stimulation (Figure 4E). CD4<sup>+</sup> T cells produced only low levels of the T<sub>H</sub>2 cell cytokine IL-4, which did not change after therapy (Figure 4E). CD8<sup>+</sup> T cells from untreated CLL patients show increased production of effector-type cytokines<sup>16</sup>. Venetoclax-obinutuzumab treatment resulted in a significantly decreased production of IFN-γ and a trend toward lower tumor necrosis factor-α production by CD8<sup>+</sup> T cells (Figure 4F). In contrast to CD8<sup>+</sup> T cells, NK cell cytokine production and degranulation are impaired in untreated CLL patients<sup>17,18</sup>. Following venetoclax-obinutuzumab treatment, degranulation, as well as IFN-γ production, of NK cells improved significantly (Figure 4G).

Together, these data demonstrate a decrease in immunosuppressive T-cell subsets, as well as restoration of T-cell and NK cell function, but not IgG production, after venetoclax-obinutuzumab treatment.

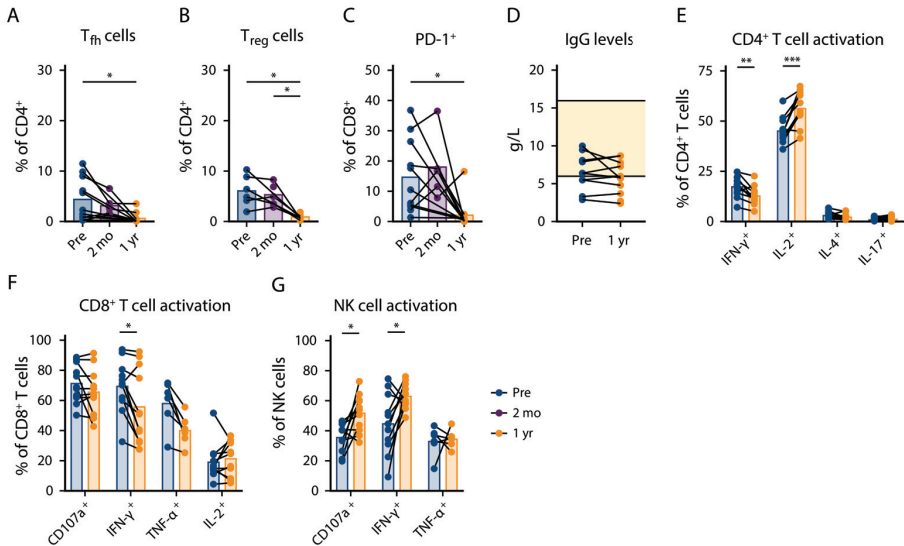


**Figure 4. Tumor-submissive T-cell subsets decrease during venetoclax-obinutuzumab treatment.** Lymphocyte analysis in PB of patients at baseline ( $n = 11$ ), after preinduction with obinutuzumab ( $n = 5$ ), and after 1 year of treatment with venetoclax-obinutuzumab ( $n = 11$ ) by flow cytometry. Percentage of  $T_{fh}$  (CXCR5<sup>+</sup>PD-1<sup>+</sup>) cells (A) and  $T_{regs}$  (CD25<sup>+</sup>FoxP3<sup>+</sup>) (B) within CD4<sup>+</sup> T cells. (C) Percentage of PD-1<sup>+</sup> cells within CD8<sup>+</sup> T cells. (D) IgG levels in plasma at baseline and after 1 year of venetoclax-obinutuzumab treatment. (E) Cytokine production by CD4<sup>+</sup> T cells after stimulation of PBMCs with PMA/ionomycin for 4 hours. Cytokine production and CD107a expression by CD8<sup>+</sup> T cells (F) and NK cells (G) after stimulation of PBMCs with PMA/ionomycin for 4 hours. \* $P < .05$ , \*\* $P < .01$ , \*\*\* $P < .001$ , 1-way ANOVA followed by Sidak's multiple-comparisons test.

### Reduction in nonmalignant lymphocytes when venetoclax is combined with ibrutinib

Current clinical studies investigate the combination of venetoclax with anti-CD20 antibodies, as well as with the BTK inhibitor ibrutinib<sup>46</sup>. We studied nonmalignant lymphocyte populations in paired samples from patients at baseline, after ibrutinib preinduction, and after ~1 year of venetoclax-ibrutinib treatment. Of note, all samples were obtained from patients who had received prior (chemotherapy-based) treatment.

Although the CLL load decreased significantly after venetoclax-ibrutinib treatment, CLL cells were still present in the PBMC fraction of most patients (mean percentage of lymphocytes,  $95.2 \pm 2.4$  vs  $8.2 \pm 12.9$ ; Supplementary Figure 5A), and 45% of patients remained MRD positive at this time point in the trial cohort.

Low healthy B-cell numbers persist during ibrutinib monotherapy, especially in patients with relapsed or refractory disease<sup>47</sup>. Also in our cohort, the percentage and absolute numbers of healthy B cells were low at baseline and decreased after 1 year of venetoclax-ibrutinib treatment (from  $8.8 \times 10^7/L \pm 6.2 \times 10^7/L$  to  $0.1 \times 10^6/L \pm 0.03 \times 10^6/L$ ; Figure 5A; Supplementary Figure 5A).

The majority (~80%) of remaining lymphocytes in the PB following venetoclax-ibrutinib treatment were T cells and NK cells (Supplementary Figure 5A). The baseline T-cell count in these previously treated patients was above the reference range in 5 of 10 patients ( $2.5 \times 10^9/L \pm 1.3 \times 10^9/L$ ). The absolute numbers of CD4<sup>+</sup> and CD8<sup>+</sup> T cells decreased significantly (approximately twofold) during venetoclax-ibrutinib treatment, but they stayed within reference values in most patients (Figure 5B). The decline was equal across T-cell subsets, because the CD4/CD8 ratio and the differentiation status of T cells did not change after treatment (Supplementary Figure 5B-D). Only Vδ2 T-cell numbers remained stable after venetoclax-ibrutinib treatment (Supplementary Figure 5E-H). The decrease in T-cell numbers was not observed after ibrutinib preinduction.

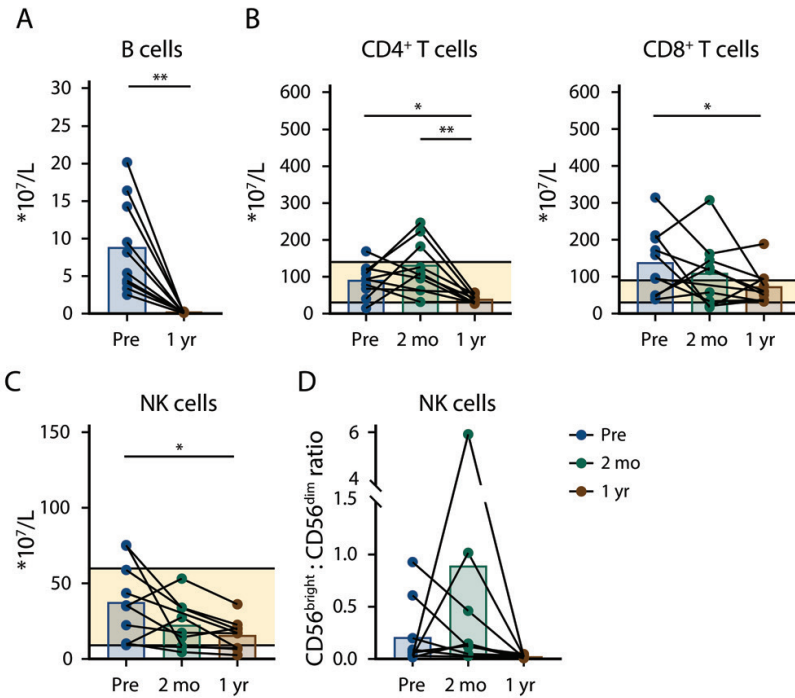


**Figure 5. Depletion of nonmalignant lymphocytes when venetoclax is combined with ibrutinib.** Lymphocyte analysis in PB of patients at baseline, after preinduction with ibrutinib, and after 1 year of treatment with venetoclax-ibrutinib (n = 10) by flow cytometry. Absolute number of B cells (A) and CD4<sup>+</sup> and CD8<sup>+</sup> T cells (B) in PB. (C) Absolute number of NK (CD56<sup>bright</sup> and CD16<sup>+</sup>) cells in PB. (D) Ratio of CD56<sup>bright</sup> (CD56<sup>bright</sup>CD16<sup>+</sup>) cells vs CD56<sup>dim</sup> (CD56<sup>dim</sup>CD16<sup>+</sup>) cells. Horizontal lines indicate reference values. \**P* < .05, \*\**P* < .01, 1-way ANOVA followed by Sidak’s multiple-comparisons test.

Similar to the T-cell compartment, the absolute number of NK cells was reduced upon 1 year of venetoclax-ibrutinib treatment (from  $37.6 \times 10^7/L \pm 25.7 \times 10^9/L$  to  $15.7 \times 10^7/L \pm 10.1 \times 10^7/L$ ; Figure 5C). The CD56<sup>bright</sup>/CD56<sup>dim</sup> ratio decreased almost 10-fold, indicating that CD56<sup>bright</sup> cells were more susceptible to treatment-induced cellular loss (Figure 5D; Supplementary Figure 5I-J). Other

than in 1 patient, the CD56<sup>bright</sup>/CD56<sup>dim</sup> ratio remained stable after preinduction with ibrutinib, indicating that the treatment-induced cell loss was caused by prolonged venetoclax-ibrutinib therapy.

In conclusion, the loss of healthy B, T, and NK cells is observed when venetoclax is used in combination with obinutuzumab or with ibrutinib.

### **Fewer T<sub>fh</sub> cells, T<sub>regs</sub>, and PD-1<sup>+</sup> CD8<sup>+</sup> T cells after treatment with venetoclax and ibrutinib**

The frequencies of T<sub>fh</sub> cells, T<sub>regs</sub>, and PD-1<sup>+</sup> CD8<sup>+</sup> T cells were reduced significantly after venetoclax-ibrutinib treatment, similar to our observations in the venetoclax-obinutuzumab cohort (Figure 6A-C). The frequency of T<sub>regs</sub> and PD-1<sup>+</sup> CD8<sup>+</sup> T cells trended downward during ibrutinib preinduction, but T<sub>fh</sub> cell numbers were significantly affected by ibrutinib monotherapy, in line with recent reports on the effects of ibrutinib on T<sub>fh</sub> cells<sup>48,49</sup>.

In accordance with low healthy B-cell numbers, plasma IgG levels did not increase after 1 year of venetoclax-ibrutinib treatment (Figure 6D). Treatment with venetoclax-ibrutinib led to significantly reduced IL-4 production by CD4<sup>+</sup> T cells, in line with previous reports on abrogated T<sub>H</sub>2 cell responses after ibrutinib in vitro (Figure 6E)<sup>26</sup>. We did not observe any clear changes in the cytokine-production profiles of CD8<sup>+</sup> T cells or Vδ2 T cells after treatment (Figure 6F; Supplementary Figure 6). The functionality of NK cells did not improve after venetoclax-ibrutinib treatment (Figure 6G).

In summary, a reduction in several immunosuppressive features of CLL is also seen in a patient cohort treated with venetoclax in combination with ibrutinib.

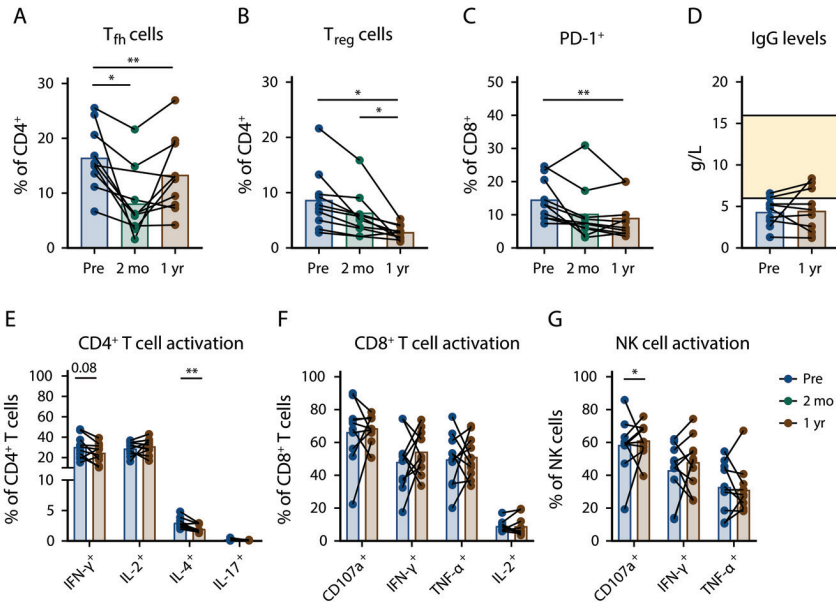


**Figure 6. Fewer T<sub>fh</sub> and PD-1<sup>+</sup>CD8<sup>+</sup>T cells after treatment with venetoclax-ibrutinib.** Lymphocyte analysis in PB of patients at baseline, after preinduction with ibrutinib, and after 1 year of treatment with venetoclax-ibrutinib (n = 10) by flow cytometry. Percentage of T<sub>fh</sub> (CXCR5<sup>+</sup>PD-1<sup>+</sup>) cells (A) and T<sub>regs</sub> (CD25<sup>+</sup>FoxP3<sup>+</sup>) (B) within CD4<sup>+</sup> T cells. (C) Percentage of PD-1<sup>+</sup> cells within CD8<sup>+</sup> T cells. (D) IgG levels in plasma at baseline and after 1 year of venetoclax-ibrutinib. (E) Cytokine production by CD4<sup>+</sup> T cells after stimulation of PBMCs with PMA/ionomycin for 4 hours. Cytokine production and CD107a expression by CD8<sup>+</sup> T cells (F) and NK cells (G) after stimulation of PBMCs with PMA/ionomycin for 4 hours. \**P* < .05, \*\**P* < .01, 1-way ANOVA followed by Sidak’s multiple-comparisons test.

**DISCUSSION**

The interplay of malignant cells with the immune system has a pivotal role in the pathobiology of CLL; it profoundly modifies nonmalignant lymphocyte subsets, resulting in suppressed tumor surveillance and a higher risk for infections and secondary malignancies. In this paired analysis, we demonstrate that nonleukemic lymphocyte alterations are even more pronounced in the LN compared with the PB of CLL patients. Venetoclax has emerged as a powerful therapeutic agent in the CLL treatment landscape, and our study shows that the immune system is reshaped during venetoclax-containing regimens, leading to a reduction in the immunosuppressive footprint of CLL.

Ex vivo studies have identified the essential role of the LN microenvironment in the induction of proliferation and suppression of apoptosis in CLL cells. Within the LN, CLL cells obtain a distinctly activated gene signature in comparison with the PB<sup>50-52</sup>. Presumably, T cells are an important source of the stimuli that CLL cells receive within the LN. CD4<sup>+</sup> T cells secrete cytokines and express costimulatory molecules that support CLL cells<sup>1,3</sup>, and T<sub>fh</sub> cells provide a source for CD40L and IL-21 that, together, induce CLL proliferation<sup>7</sup>. We observed that CD4<sup>+</sup> T cells are abundant in the

LN of CLL patients and that  $T_{fh}$  cells make up a large proportion of the  $CD4^+$  T cells surrounding the CLL cells in the LN.

In addition to strengthening the concept that the LN provides a CLL stimulatory environment, our data indicate it to be a protective niche from immunosurveillance. The numbers of NK and  $CD8^+$  T cells are relatively low, as well as  $V\delta 1$  and  $V\delta 2$  T-cell numbers, both of which have cytotoxic properties against CLL cells<sup>53,54</sup>. Moreover, high PD-1 expression on  $CD8^+$  T cells fits with an immunosuppressed profile in the LN. The increased numbers of  $T_{regs}$  in the LN that we and other investigators describe likely suppress cellular immune responses within the LN<sup>55</sup>. Therefore, the disappointing efficacy of cellular-based therapies may improve when such treatment modalities are combined with agents that displace CLL cells from the LN, as is seen in early clinical studies with ibrutinib and chimeric antigen receptor T cells<sup>56</sup>.

The numbers of nonmalignant lymphocytes decreased during venetoclax-based treatment, although they generally remained within the normal range. Direct and indirect effects of venetoclax treatment may explain the decrease in nonmalignant lymphocytes, although caution is required when determining the effect of venetoclax itself because of the combination treatments administered in both cohorts. Within the venetoclax-obinutuzumab cohort, the depletion of B cells and NK cells may be attributed, at least in part, to obinutuzumab, and we indeed observe depletion of B cells and NK cells after preinduction with obinutuzumab. Normally, NK cell counts have largely recovered 3 months after obinutuzumab monotherapy, suggesting an additional role for venetoclax<sup>45</sup>. Because a similar pattern is seen in the ibrutinib-venetoclax cohort, there is a possibility that venetoclax affects healthy lymphocyte counts. During ibrutinib monotherapy, elevated and reduced T-cell numbers have been described<sup>23,27,57</sup>, whereas we have not seen alterations in NK cell numbers in previous analyses in a mixed cohort (I.d.W. and A.P.K., unpublished data). In both cohorts, preinduction with obinutuzumab or ibrutinib had no significant effect on T-cell counts, indicating that venetoclax has the largest effect on T-cell numbers.

The fact that lymphocyte counts decline across all subtypes in both cohorts might indicate that healthy lymphocyte survival depends on Bcl-2 to a greater extent than previously assumed. Whereas  $CD4^+$  T-cell numbers decreased across all subsets, this was particularly true for  $T_{regs}$ . High levels of Noxa make  $T_{regs}$  more prone to apoptosis, which in CLL  $T_{regs}$  is counterbalanced by elevated Bcl-2 levels, perhaps contributing to their venetoclax sensitivity<sup>58</sup>.

The depletion of CLL cells by venetoclax-containing regimens can also diminish the microenvironmental stimuli that recruit and support T cells and NK cells. Although there is no definitive proof for CLL-specific T-cell clones, the consistent elevation of T-cell numbers and skewed T-cell receptor repertoire suggest their existence, and such clones may disappear when no longer receiving CLL-derived antigenic stimulation<sup>5,59</sup>. Considering the active recruitment of a supportive immune environment by CLL, the loss of CLL cells could directly and indirectly deprive T cells and NK cells of cytokines and costimulation.



Similarly, the elimination of CLL cells may contribute to the decline of the tumor-submissive T-cell state. The decrease in exhaustion markers and T<sub>reg</sub> numbers is also seen following treatment with ibrutinib, supporting the hypothesis that this is CLL dependent rather than treatment drug dependent<sup>23,27</sup>.

Fludarabine has profound detrimental effects on T-cell numbers, and immune recovery of T cells takes >6 months, leading to an extended period of increased infection risk<sup>20,21</sup>. Now that discontinuation of venetoclax-based treatments upon reaching deep remissions appears to be feasible<sup>29-31</sup>, it is of clinical relevance to assess whether lymphocyte counts recover after cessation, especially if the decrease in nonmalignant lymphocytes is a direct effect of venetoclax. Despite the commonly observed neutropenia, venetoclax treatment is not associated with an increased infection risk so far<sup>60</sup>, which may be explained by our data that venetoclax treatment does not lead to reduced functionality of T cells and NK cells.

Cellular-based immunotherapy has disappointing responses in CLL, which may be related to the acquired T-cell dysfunction<sup>61-64</sup>. The disruption of the immunosuppressive state and the improved lymphocyte functionality that we observe after venetoclax-based therapy may improve the efficacy of cellular-based therapies for CLL. Future studies should investigate the effect of venetoclax combination treatment on nonmalignant lymphocytes in relation to sequential or combinatorial cellular-based therapy.

Taken together, our data show that changes in nonleukemic lymphocytes are more pronounced in the LN of CLL patients compared with in the PB. In addition to effectively depleting CLL cells, venetoclax-based therapy is accompanied by extensive changes in the immune system. Treatment regimens with venetoclax in combination with obinutuzumab or ibrutinib result in reduced numbers of healthy lymphocytes, but the immunological footprint and suppressive features of the CLL immune system decline during venetoclax-based treatment.

## **ACKNOWLEDGEMENTS**

The authors thank the patients and HCs for their blood and LN samples, as well as Antoinet Schoonderwoerd for assistance.

## REFERENCES

1. Forconi F, Moss P. Perturbation of the normal immune system in patients with CLL. *Blood*. 2015;126(5):573-81.
2. Riches JC, Gribben JG. Understanding the immunodeficiency in chronic lymphocytic leukemia: potential clinical implications. *Hematol Oncol Clin North Am*. 2013;27(2):207-35.
3. van Attekum MH, Eldering E, Kater AP. Chronic lymphocytic leukemia cells are active participants in microenvironmental cross-talk. *Haematologica*. 2017;102(9):1469-76.
4. Burger JA, Quiroga MP, Hartmann E, et al. High-level expression of the T-cell chemokines CCL3 and CCL4 by chronic lymphocytic leukemia B cells in nurselike cell cocultures and after BCR stimulation. *Blood*. 2009;113(13):3050-8.
5. Mackus WJ, Frakking FN, Grummels A, et al. Expansion of CMV-specific CD8+CD45RA+CD27- T cells in B-cell chronic lymphocytic leukemia. *Blood*. 2003;102(3):1057-63.
6. Mu X, Kay NE, Gosland MP, Jennings CD. Analysis of blood T-cell cytokine expression in B-chronic lymphocytic leukaemia: evidence for increased levels of cytoplasmic IL-4 in resting and activated CD8 T cells. *Br J Haematol*. 1997;96(4):733-5.
7. Pascutti MF, Jak M, Tromp JM, et al. IL-21 and CD40L signals from autologous T cells can induce antigen-independent proliferation of CLL cells. *Blood*. 2013;122(17):3010-9.
8. Catakovic K, Gassner FJ, Ratswohl C, et al. TIGIT expressing CD4+T cells represent a tumor-supportive T cell subset in chronic lymphocytic leukemia. *Oncoimmunology*. 2017;7(1):e1371399.
9. Saulep-Easton D, Vincent FB, Quah PS, et al. The BAFF receptor TACI controls IL-10 production by regulatory B cells and CLL B cells. *Leukemia*. 2016;30(1):163-72.
10. Jitschin R, Braun M, Buttner M, et al. CLL-cells induce IDOhi CD14+HLA-DRlo myeloid-derived suppressor cells that inhibit T-cell responses and promote TRegs. *Blood*. 2014;124(5):750-60.
11. Hanna BS, Roessner PM, Scheffold A, et al. PI3Kdelta inhibition modulates regulatory and effector T-cell differentiation and function in chronic lymphocytic leukemia. *Leukemia*. 2018.
12. D'Arena G, Laurenti L, Minervini MM, et al. Regulatory T-cell number is increased in chronic lymphocytic leukemia patients and correlates with progressive disease. *Leuk Res*. 2011;35(3):363-8.
13. Gorgun G, Holderried TA, Zahrieh D, Neuberger D, Gribben JG. Chronic lymphocytic leukemia cells induce changes in gene expression of CD4 and CD8 T cells. *J Clin Invest*. 2005;115(7):1797-805.
14. Ramsay AG, Johnson AJ, Lee AM, et al. Chronic lymphocytic leukemia T cells show impaired immunological synapse formation that can be reversed with an immunomodulating drug. *J Clin Invest*. 2008;118(7):2427-37.
15. Ramsay AG, Clear AJ, Fatah R, Gribben JG. Multiple inhibitory ligands induce impaired T-cell immunologic synapse function in chronic lymphocytic leukemia that can be blocked with lenalidomide: establishing a reversible immune evasion mechanism in human cancer. *Blood*. 2012;120(7):1412-21.
16. Riches JC, Davies JK, McClanahan F, et al. T cells from CLL patients exhibit features of T-cell exhaustion but retain capacity for cytokine production. *Blood*. 2013;121(9):1612-21.
17. Parry HM, Stevens T, Oldreive C, et al. NK cell function is markedly impaired in patients with chronic lymphocytic leukaemia but is preserved in patients with small lymphocytic lymphoma. *Oncotarget*. 2016;7(42):68513-26.
18. MacFarlane AWt, Jillab M, Smith MR, et al. NK cell dysfunction in chronic lymphocytic leukemia is associated with loss of the mature cells expressing inhibitory killer cell Ig-like receptors. *Oncoimmunology*. 2017;6(7):e1330235.
19. Rimsza LM, Jaramillo MC. Indolent lymphoma: follicular lymphoma and the microenvironment-insights from gene expression profiling. *Hematology Am Soc Hematol Educ Program*. 2014;2014(1):163-8.

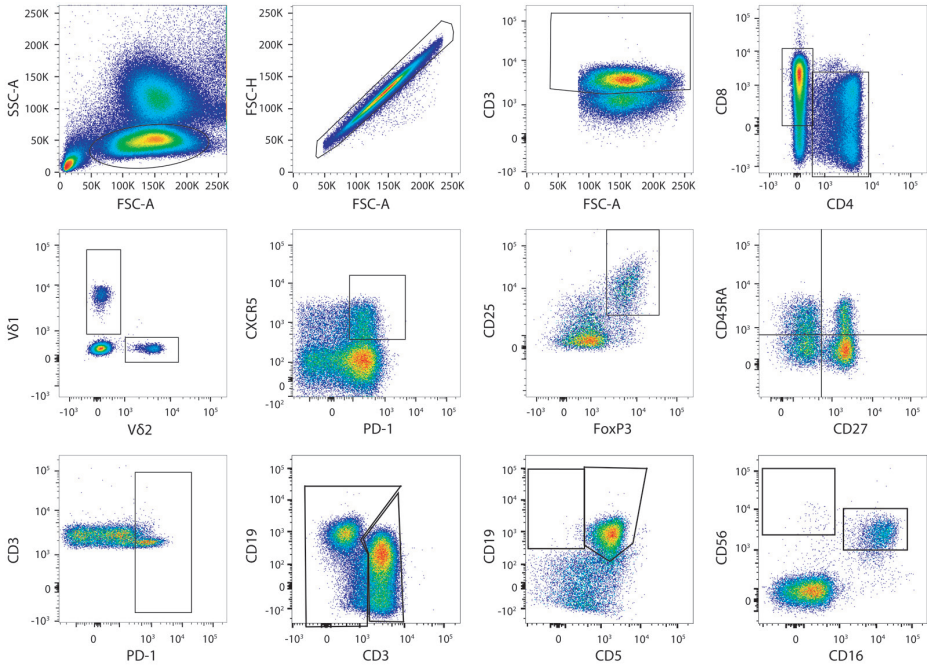
20. Tam CS, O'Brien S, Wierda W, et al. Long-term results of the fludarabine, cyclophosphamide, and rituximab regimen as initial therapy of chronic lymphocytic leukemia. *Blood*. 2008;112(4):975-80.
21. Ysebaert L, Gross E, Kuhlein E, et al. Immune recovery after fludarabine-cyclophosphamide-rituximab treatment in B-chronic lymphocytic leukemia: implication for maintenance immunotherapy. *Leukemia*. 2010;24(7):1310-6.
22. Pleyer C, Wiestner A, Sun C. Immunological changes with kinase inhibitor therapy for chronic lymphocytic leukemia. *Leuk Lymphoma*. 2018;59(12):2792-800.
23. Niemann CU, Herman SE, Maric I, et al. Disruption of in vivo Chronic Lymphocytic Leukemia Tumor-Microenvironment Interactions by Ibrutinib--Findings from an Investigator-Initiated Phase II Study. *Clin Cancer Res*. 2016;22(7):1572-82.
24. Kohrt HE, Sagiv-Barfi I, Rafiq S, et al. Ibrutinib antagonizes rituximab-dependent NK cell-mediated cytotoxicity. *Blood*. 2014;123(12):1957-60.
25. Stiff A, Trikha P, Wesolowski R, et al. Myeloid-Derived Suppressor Cells Express Bruton's Tyrosine Kinase and Can Be Depleted in Tumor-Bearing Hosts by Ibrutinib Treatment. *Cancer Res*. 2016;76(8):2125-36.
26. Dubovsky JA, Beckwith KA, Natarajan G, et al. Ibrutinib is an irreversible molecular inhibitor of ITK driving a Th1-selective pressure in T lymphocytes. *Blood*. 2013;122(15):2539-49.
27. Long M, Beckwith K, Do P, et al. Ibrutinib treatment improves T cell number and function in CLL patients. *J Clin Invest*. 2017;127(8):3052-64.
28. Roberts AW, Davids MS, Pagel JM, et al. Targeting BCL2 with Venetoclax in Relapsed Chronic Lymphocytic Leukemia. *N Engl J Med*. 2016;374(4):311-22.
29. Seymour JF, Kipps TJ, Eichhorst B, et al. Venetoclax-Rituximab in Relapsed or Refractory Chronic Lymphocytic Leukemia. *N Engl J Med*. 2018;378(12):1107-20.
30. Kater AP, Kersting S, van Norden Y, et al. Obinutuzumab pretreatment abrogates tumor lysis risk while maintaining undetectable MRD for venetoclax + obinutuzumab in CLL. *Blood Adv*. 2018;2(24):3566-71.
31. Fischer K, Al-Sawaf O, Fink AM, et al. Venetoclax and obinutuzumab in chronic lymphocytic leukemia. *Blood*. 2017;129(19):2702-5.
32. Flinn IW, Gribben JG, Dyer MJS, et al. Phase 1b study of venetoclax-obinutuzumab in previously untreated and relapsed/refractory chronic lymphocytic leukemia. *Blood*. 2019.
33. Zhan Y, Carrington EM, Zhang Y, Heinzl S, Lew AM. Life and Death of Activated T Cells: How Are They Different from Naive T Cells? *Front Immunol*. 2017;8:1809.
34. Carrington EM, Zhan Y, Brady JL, et al. Anti-apoptotic proteins BCL-2, MCL-1 and A1 summate collectively to maintain survival of immune cell populations both in vitro and in vivo. *Cell Death Differ*. 2017;24(5):878-88.
35. Teh BW, Tam CS, Handunnetti S, Worth LJ, Slavin MA. Infections in patients with chronic lymphocytic leukaemia: Mitigating risk in the era of targeted therapies. *Blood Rev*. 2018;32(6):499-507.
36. Hilal T, Gea-Banacloche JC, Leis JF. Chronic lymphocytic leukemia and infection risk in the era of targeted therapies: Linking mechanisms with infections. *Blood Rev*. 2018;32(5):387-99.
37. Remmerswaal EB, Havenith SH, Idu MM, et al. Human virus-specific effector-type T cells accumulate in blood but not in lymph nodes. *Blood*. 2012;119(7):1702-12.
38. Hallaert DY, Jaspers A, van Noesel CJ, van Oers MH, Kater AP, Eldering E. c-Abl kinase inhibitors overcome CD40-mediated drug resistance in CLL: implications for therapeutic targeting of chemoresistant niches. *Blood*. 2008;112(13):5141-9.
39. Stolk D, van der Vliet HJ, de Gruijl TD, van Kooyk Y, Exley MA. Positive & Negative Roles of Innate Effector Cells in Controlling Cancer Progression. *Front Immunol*. 2018;9:1990.
40. Moretta L. Dissecting CD56dim human NK cells. *Blood*. 2010;116(19):3689-91.

41. Wan Z, Lin Y, Zhao Y, Qi H. TFH cells in bystander and cognate interactions with B cells. *Immunol Rev.* 2019;288(1):28-36.
42. Cha Z, Zang Y, Guo H, et al. Association of peripheral CD4+ CXCR5+ T cells with chronic lymphocytic leukemia. *Tumour Biol.* 2013;34(6):3579-85.
43. Qiu L, Zhou Y, Yu Q, Zheng S, Wang Z, Huang Q. Elevated levels of follicular T helper cells and their association with therapeutic effects in patients with chronic lymphocytic leukaemia. *Immunol Lett.* 2018;197:15-28.
44. Mahnke YD, Brodie TM, Sallusto F, Roederer M, Lugli E. The who's who of T-cell differentiation: human memory T-cell subsets. *Eur J Immunol.* 2013;43(11):2797-809.
45. Garcia-Munoz R, Aguinaga L, Feliu J, et al. Obinutuzumab induces depletion of NK cells in patients with chronic lymphocytic leukemia. *Immunotherapy.* 2018;10(6):491-9.
46. Jain N, Keating MJ, Thompson PA, et al. Combined Ibrutinib and Venetoclax in Patients with Treatment-Naïve High-Risk Chronic Lymphocytic Leukemia (CLL). *Blood.* 2018;132:696-.
47. Sun C, Tian X, Lee YS, et al. Partial reconstitution of humoral immunity and fewer infections in patients with chronic lymphocytic leukemia treated with ibrutinib. *Blood.* 2015;126(19):2213-9.
48. Sahaf B, Tebaykin D, Hopper M, et al. Ibrutinib Inhibits cGVHD Pathogenic Pre-Germinal Center B-Cells and Follicular Helper Cells While Preserving Immune Memory and Th1 T-Cells. *Blood.* 2017;130(Suppl 1):4481-.
49. Marshall AJ, Zhang C, Hou S, Wu X. Abnormal T follicular helper cell subsets in Chronic Lymphocytic Leukemia. *J Immunol.* 2018;200(1 Supplement):166.28-.28.
50. Herishanu Y, Perez-Galan P, Liu D, et al. The lymph node microenvironment promotes B-cell receptor signaling, NF-kappaB activation, and tumor proliferation in chronic lymphocytic leukemia. *Blood.* 2011;117(2):563-74.
51. Herndon TM, Chen SS, Saba NS, et al. Direct in vivo evidence for increased proliferation of CLL cells in lymph nodes compared to bone marrow and peripheral blood. *Leukemia.* 2017;31(6):1340-7.
52. Pasikowska M, Walsby E, Apollonio B, et al. Phenotype and immune function of lymph node and peripheral blood CLL cells are linked to transendothelial migration. *Blood.* 2016;128(4):563-73.
53. Siegers GM, Dhamko H, Wang XH, et al. Human Vdelta1 gammadelta T cells expanded from peripheral blood exhibit specific cytotoxicity against B-cell chronic lymphocytic leukemia-derived cells. *Cytotherapy.* 2011;13(6):753-64.
54. de Weerd I, Hofland T, Lameris R, et al. Improving CLL Vgamma9Vdelta2-T-cell fitness for cellular therapy by ex vivo activation and ibrutinib. *Blood.* 2018;132(21):2260-72.
55. Lad DP, Varma S, Varma N, Sachdeva MU, Bose P, Malhotra P. Regulatory T-cells in B-cell chronic lymphocytic leukemia: their role in disease progression and autoimmune cytopenias. *Leuk Lymphoma.* 2013;54(5):1012-9.
56. Fraietta JA, Beckwith KA, Patel PR, et al. Ibrutinib enhances chimeric antigen receptor T-cell engraftment and efficacy in leukemia. *Blood.* 2016;127(9):1117-27.
57. Yin Q, Sivina M, Robins H, et al. Ibrutinib Therapy Increases T Cell Repertoire Diversity in Patients with Chronic Lymphocytic Leukemia. *J Immunol.* 2017;198(4):1740-7.
58. Jak M, Mous R, Remmerswaal EB, et al. Enhanced formation and survival of CD4+ CD25hi Foxp3+ T-cells in chronic lymphocytic leukemia. *Leuk Lymphoma.* 2009;50(5):788-801.
59. Vardi A, Agathangelidis A, Stalika E, et al. Antigen Selection Shapes the T-cell Repertoire in Chronic Lymphocytic Leukemia. *Clin Cancer Res.* 2016;22(1):167-74.

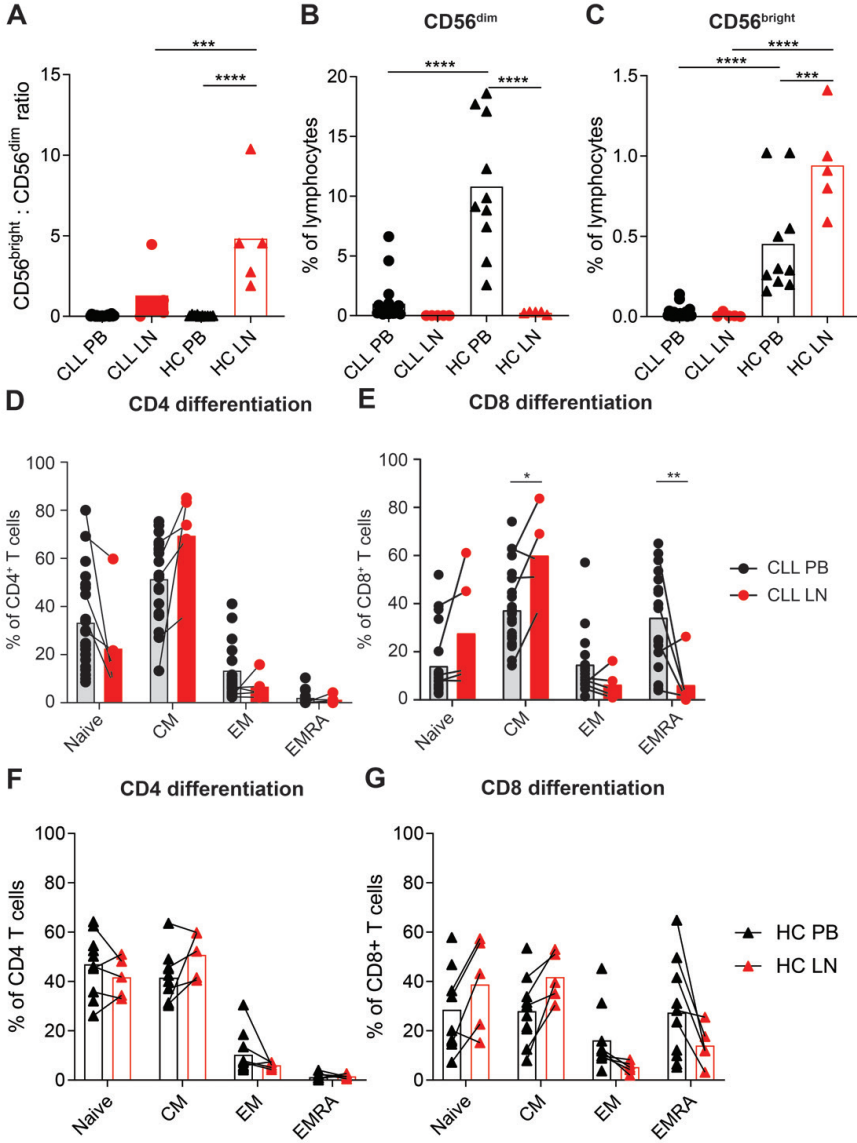
## CHAPTER 5

60. Davids MS, Hallek M, Wierda W, et al. Comprehensive Safety Analysis of Venetoclax Monotherapy for Patients with Relapsed/Refractory Chronic Lymphocytic Leukemia. *Clin Cancer Res*. 2018;24(18):4371-9.
61. Lorentzen CL, Straten PT. CD19-Chimeric Antigen Receptor T Cells for Treatment of Chronic Lymphocytic Leukaemia and Acute Lymphoblastic Leukaemia. *Scandinavian journal of immunology*. 2015;82(4):307-19.
62. Turtle CJ, Hay KA, Hanafi LA, et al. Durable Molecular Remissions in Chronic Lymphocytic Leukemia Treated With CD19-Specific Chimeric Antigen Receptor-Modified T Cells After Failure of Ibrutinib. *J Clin Oncol*. 2017;35(26):3010-20.
63. Geyer MB, Brentjens RJ. Review: Current clinical applications of chimeric antigen receptor (CAR) modified T cells. *Cytotherapy*. 2016;18(11):1393-409.
64. Porter DL, Hwang WT, Frey NV, et al. Chimeric antigen receptor T cells persist and induce sustained remissions in relapsed refractory chronic lymphocytic leukemia. *Sci Transl Med*. 2015;7(303):303ra139.

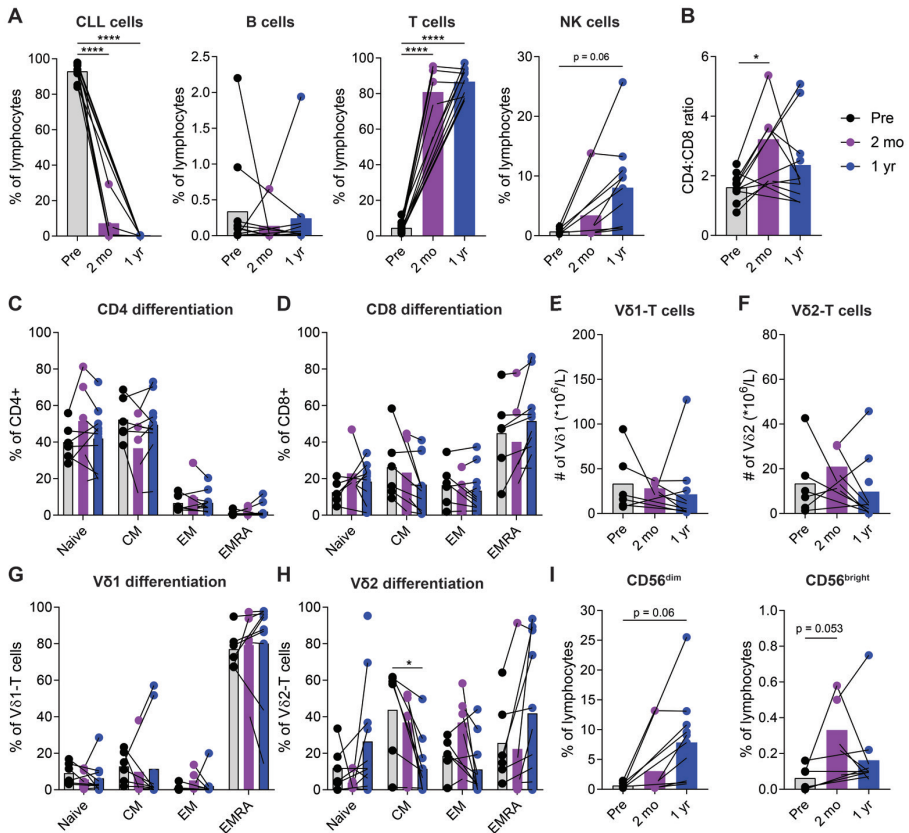
**SUPPLEMENTARY DATA**



**Supplementary Figure 1. Gating strategy of immune cell subsets.** Gating strategy used for the analysis of immune cell composition. Top row, from left to right: gating of lymphocytes, single cells, CD3<sup>+</sup> T cells, CD4<sup>+</sup> and CD8<sup>+</sup> T cells, and Vδ1 and Vδ2 T cells. Middle row, from left to right: gating of CXCR5<sup>+</sup>PD-1<sup>+</sup> T<sub>fh</sub> cells within CD4<sup>+</sup> T cells, CD25<sup>+</sup>FoxP3<sup>+</sup> T<sub>regs</sub> within CD4<sup>+</sup> T cells, differentiation of CD8<sup>+</sup> T cells, and PD-1<sup>+</sup> CD8<sup>+</sup> T cells. Bottom row, from left to right: gating of CD3<sup>-</sup> lymphocytes, CD19<sup>+</sup>CD5<sup>+</sup> CLL cells and CD19<sup>+</sup>CD5<sup>-</sup> healthy B cells within CD3<sup>-</sup> gate, and CD56<sup>+</sup>CD16<sup>+/-</sup> NK cells within the CD3<sup>-</sup> gate.



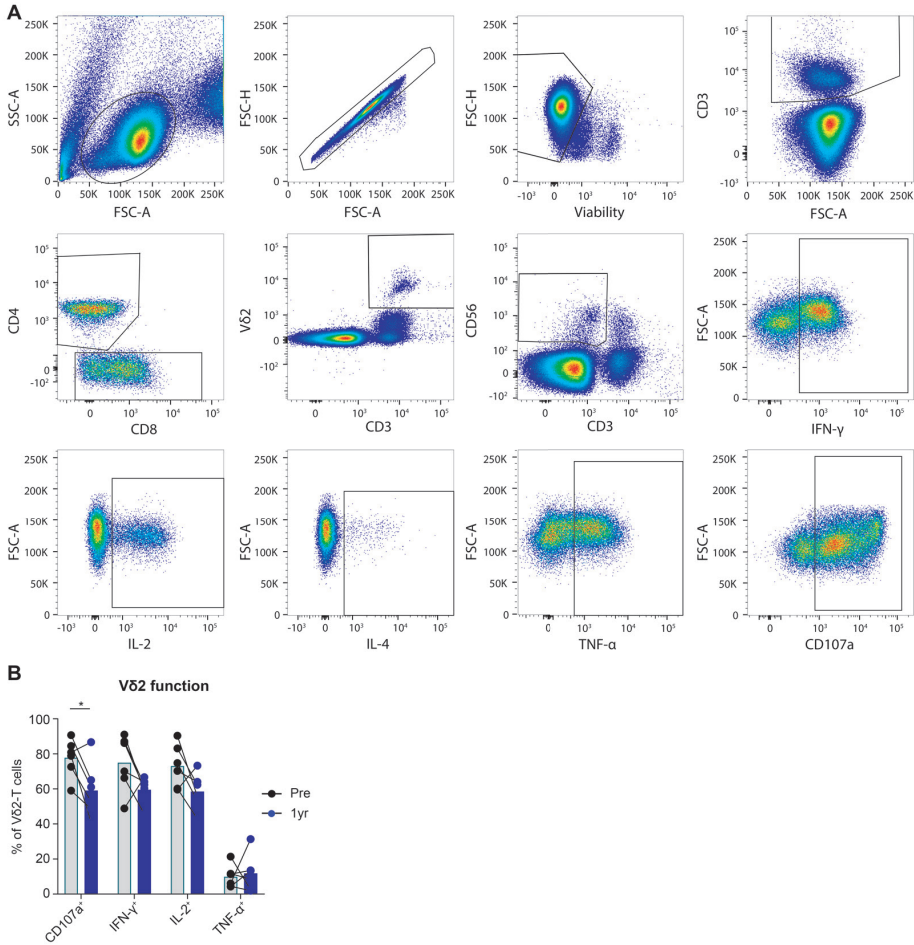
**Supplementary Figure 2. CLL cells evade cytotoxic NK cells in the lymph node.** Lymphocyte analysis in PB and LN samples from untreated CLL patients (PB: n=42, LN: n=28) and HCs (PB: n=10, LN: n=5) by flow cytometry. (A) Ratio of CD56<sup>bright</sup> (CD56<sup>bright</sup>CD16<sup>-</sup>) versus CD56<sup>dim</sup> (CD56<sup>dim</sup>CD16<sup>+</sup>), (B) percentage of CD56<sup>dim</sup> (CD56<sup>dim</sup>CD16<sup>+</sup>) and (C) percentage of CD56<sup>bright</sup> (CD56<sup>bright</sup>CD16<sup>-</sup>) cells within lymphocytes. Differentiation of (D) CD4<sup>+</sup> T cells from CLL patients (PB: n=21, LN: n=5), (E) CD8<sup>+</sup> T cells from CLL patients (PB: n=21, LN: n=5), (F) CD4<sup>+</sup> T cells from HCs (PB: n=10, LN: n=5) and (G) CD8<sup>+</sup> T cells from HCs (PB: n=10, LN: n=5) based on CD27 and CD45RA expression. Naive: CD27<sup>+</sup>CD45RA<sup>+</sup>; CM: CD27<sup>+</sup>CD45RA<sup>-</sup>; EM: CD27<sup>-</sup>CD45RA<sup>+</sup>; EMRA: CD27<sup>-</sup>CD45RA<sup>-</sup> (n=5). Data are presented as mean (bar) and individual patients (dots). \**P* < 0.05; \*\**P* < 0.01; \*\*\**P* < 0.001, \*\*\*\**P* < 0.0001 (A-C: one-way ANOVA followed by Sidak’s multiple comparisons test, D-G: one-way ANOVA followed by Holm-Sidak’s multiple comparisons test).



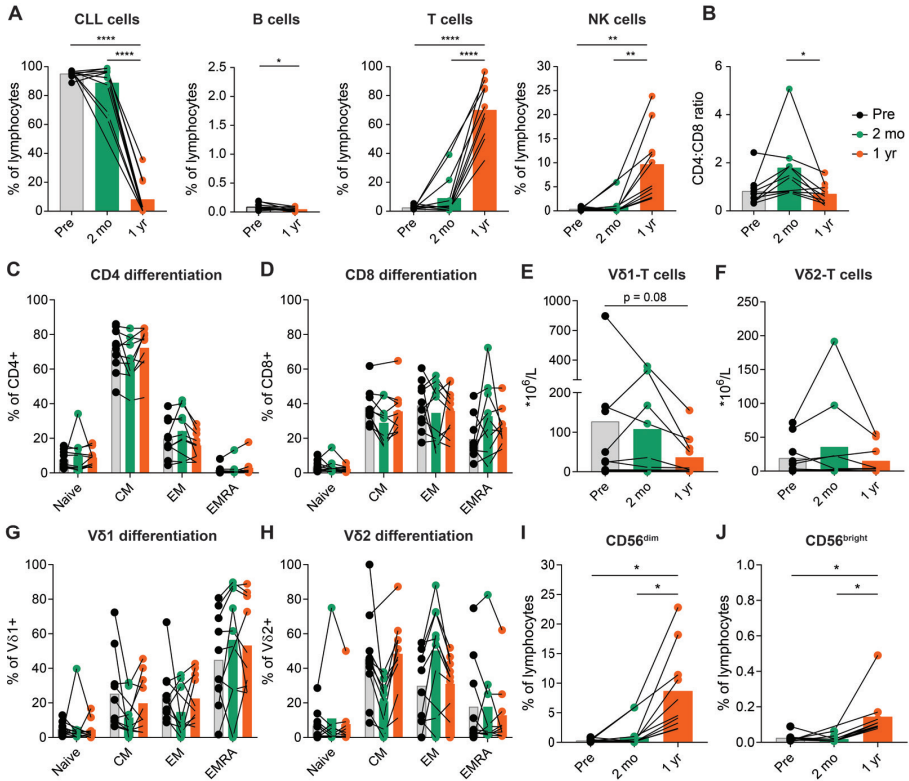
**Supplementary Figure 3. Depletion of T and NK cells during venetoclax and obinutuzumab treatment.**

Lymphocyte analysis in PB of patients at baseline (n=11), after pre-induction with obinutuzumab (n=5), and after 1 year of treatment with venetoclax-obinutuzumab (n=11) by flow cytometry. (A) Percentage of CLL (CD5<sup>+</sup>CD19<sup>+</sup>), B (CD5<sup>+</sup>CD19<sup>+</sup>), T (CD3<sup>+</sup>) and NK (CD56<sup>bright</sup> or CD16<sup>+</sup>) cells within lymphocytes. (B) Ratio of CD4<sup>+</sup> versus CD8<sup>+</sup> T cells. Differentiation of (C) CD4<sup>+</sup> and (D) CD8<sup>+</sup> T cells based on CD27 and CD45RA expression. Naive: CD27<sup>+</sup>CD45RA<sup>+</sup>, CM: CD27<sup>+</sup>CD45RA<sup>-</sup>, EM: CD27<sup>-</sup>CD45RA<sup>+</sup>, EMRA: CD27<sup>-</sup>CD45RA<sup>-</sup>. Frequency of (E) Vδ1<sup>+</sup> and (F) Vδ2<sup>+</sup> cells. Differentiation of (G) Vδ1- and (H) Vδ2- T cells based on CD27 and CD45RA expression as in (C) and (D). Percentage of (I) CD56<sup>dim</sup> (CD56<sup>dim</sup>CD16<sup>+</sup>) and CD56<sup>bright</sup> (CD56<sup>bright</sup>CD16<sup>-</sup>) cells within lymphocytes. \**P*<0.05, \*\*\*\**P*<0.0001 (one-way ANOVA followed by Holm-Sidak's multiple comparisons test).

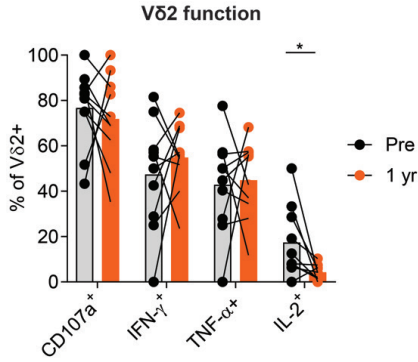




**Supplementary Figure 4. V62-T cell function during venetoclax-obinutuzumab treatment.** (A) Gating strategy of cytokine production by immune cells after PMA/ionomycin stimulation. Top row, from left to right: gating of lymphocytes, single cells, live cells, and CD3<sup>+</sup> T cells. Middle row, from left to right: gating of CD4<sup>+</sup> and CD8<sup>+</sup> T cells, V62 T cells, and CD56<sup>+</sup>CD3<sup>-</sup> NK cells. Bottom row, from left to right: gating of IFNγ, IL-2, IL-4, TNFα and CD107a positive events. (B) Lymphocyte analysis in PB of patients at baseline and after 1 year of treatment with venetoclax-obinutuzumab by flow cytometry (n=11). Cytokine production by V62-T cells after stimulation of PBMCs with PMA/ionomycin for 4 hours. \*P < 0.05 (paired t-test).



**Supplementary Figure 5. Depletion of T and NK cells when venetoclax is combined with ibrutinib.** Lymphocyte analysis in PB of patients at baseline and after 1 year of treatment with venetoclax-ibrutinib by flow cytometry (n=10). (A) Percentage of CLL (CD5<sup>+</sup>CD19<sup>+</sup>), B (CD5<sup>+</sup>CD19<sup>+</sup>), T (CD3<sup>+</sup>) and NK (CD56<sup>bright</sup> or CD16<sup>+</sup>) cells within lymphocytes. (B) Ratio of CD4<sup>+</sup> versus CD8<sup>+</sup> T cells. Differentiation of (C) CD4<sup>+</sup> and (D) CD8<sup>+</sup> T cells based on CD27 and CD45RA expression. Naive: CD27<sup>+</sup>CD45RA<sup>-</sup>, CM: CD27<sup>+</sup>CD45RA<sup>+</sup>, EM: CD27<sup>-</sup>CD45RA<sup>-</sup>, EMRA: CD27<sup>-</sup>CD45RA<sup>+</sup>. Frequency of (E) Vδ1<sup>+</sup> and (F) Vδ2<sup>+</sup> cells. Differentiation of (G) Vδ1- and (H) Vδ2-T cells based on CD27 and CD45RA expression as in (C) and (D). Percentage of (I) CD56<sup>dim</sup> (CD56<sup>dim</sup>CD16<sup>+</sup>) and (J) CD56<sup>bright</sup> (CD56<sup>bright</sup>CD16<sup>+</sup>) cells within lymphocytes. \**P* < 0.05; \*\**P* < 0.01, \*\*\*\**P* < 0.0001 (one-way ANOVA followed by Sidak's multiple comparisons test).



**Supplementary Figure 6. Vδ2-T cell function during venetoclax-ibrutinib treatment.** Lymphocyte analysis in PB of patients at baseline and after 1 year of treatment with venetoclax-ibrutinib by flow cytometry (n=10). Cytokine production by Vδ2-T cells after stimulation of PBMCs with PMA/ionomycin for 4 hours. \**P* <0.05 (paired t-test).

**Supplemental Table 1.** List of monoclonal antibodies used in this study.

HOVON139	HC HOVON141	Activation	Antibodies	Fluorochrome	Clone	Company	Catalogue number
X			CD3	PerCPCy5.5	SK7	BD Biosciences	332771
x			CD3	APC	SK7	BD Biosciences	345767
x			CD4	Pacific Blue	RPA-T4	Biolegend	300524
x			CD5	PerCPCy5.5	L17F12	BD Biosciences	341109
x			CD8	APC-H7	SK1	BD Biosciences	560273
x			CD8	PE	RPA-T8	BD Biosciences	561949
x			CD14	APC	MfP9	BD Biosciences	345787
x			CD15	eFluor450	MMA	eBioscience	48-0158- 41
x			CD16	APC	B73.1	BD Biosciences	561304
x			CD19	FITC	HIB19	BD Biosciences	555412
x			CD19	PECy7	J3-119	Beckman Coulter	IM3628
x			CD20	APC-H7	L27	BD Biosciences	641414
x	x		CD25	PE	2A3	BD Biosciences	341011
x			CD27	APC	L128	BD Biosciences	337169
x			CD33	PE	P67,6	BD Biosciences	345799
x			CD45	v500-c	2D1	BD Biosciences	655873
x			CD45RA	PE-Cy7	L48	BD Biosciences	337186
x			CD56	PE	C5.9	Cytognos	CYT-56PE
x			CD57	FITC	HNK-1	BD Biosciences	333169
x			CD154	PE	89-76	BD Biosciences	340477
x			CD185	APC	51505	R&D Systems	FAB190A
x	x		CD279	PECy7	EH12.1	BD Biosciences	561272

*Supplemental Table 1. Continued*

HOVON139	HC HOVON141	Activation	Antibodies	Fluorochrome	Clone	Company	Catalogue number
x	x		CD184	PECy7	12G5	BioLegend	306513
x			HLA-DR	PECy7	L243	BD Biosciences	335830
x			IgD	FITC	IA6-2	BD Biosciences	555778
x			Igκ	PE	Polyclonal	Cytognos	CYT- KAPPPE
x			Igλ	FITC	Polyclonal	Cytognos	CYT- LAMBF
x			TCRγδ	PECy7	11F2	BD Biosciences	655410
x			Vδ1 TCR	APC Vio770	REA-173	Miltenyi Biotec	130-100- 521
x			Vδ2 TCR	FITC	B6	BD Biosciences	562088
	x		CD185	BUV395	RF8B2	BD Biosciences	740266
	x		Vδ1 TCR	FITC	REA-173	Miltenyi Biotec	130-118- 498
	x		CD27	PerCPeF710	O323	eBioscience	46-0279- 42
	x		Vδ2 TCR	VioBright	123R3	Miltenyi Biotec	130-101- 157
	x		CD3	V500	UCHT1	BD Biosciences	561416
	x		CD45RA	BV650	HI100	BD Biosciences	563953
	x	x	CD8	BV786	RPA-T8	BD Biosciences	563823
	x		CD4	AF594	RPA-T4	Biolegend	300544
	x		FoxP3	APC	PCH101	eBioscience	17-4776- 73
	x	x	CD56	BUV395	NCAM16.2	BD Biosciences	563554
	x		CD5	PerCPeF710	UCHT2	BD Biosciences	300619
	x		Bcl-2	BV421	100	Biolegend	658709
	x		CD3	V500	UCHT1	BD Biosciences	561416
	x		Bcl-xL	PE	54H6	Cell Signaling	138355

Supplemental Table 1. Continued

HOVON139	HC HOVON141	Activation	Antibodies	Fluorochrome	Clone	Company	Catalogue number
	x		CD16	ECD	3G8	Beckman Coulter	B49216
	x		CD19	AF700	HIB19	BD Biosciences	557921
		x	CD3	BUV496	UCHT1	BD Biosciences	564809
		x	CD107a	FITC	eBioH4A3	eBioscience	11-1079- 42
		x	CD4	PerCPeF710	SK3	eBioscience	46-0047- 42
		x	IFN- $\gamma$	BV421	B27	BD Biosciences	562988
		x	V $\delta$ 2 TCR	BV711	B6	Biolegend	331411
		x	IL-17	PE	eBio64DEC17	eBioscience	12-7179- 42
		x	IL-2	PE/Dazzle 594	JES6-5H4	Biolegend	500343
		x	NKG2D	PECy7	1D11	Sony	2204060
		x	IL-4	AF647	8D4-8	Biolegend	500712
		x	TNF- $\alpha$	AF700	MAB11	BD Biosciences	557996
		x	CD69	APC/Fire 750	FN50	Biolegend	310946